ACADEMIC PRESS

Available online at www.sciencedirect.com
SCIENCE DIRECT®

NeuroImage

NeuroImage 18 (2003) 813–826

www.elsevier.com/locate/ynimg

Comparison of fMRI activation at 3 and 1.5 T during perceptual, cognitive, and affective processing

B. Krasnow,[a] L. Tamm,[a] M.D. Greicius,[a] T.T. Yang,[a] G.H. Glover,[b] A.L. Reiss,[a] and V. Menon[a,c,d,*]

[a] *Department of Psychiatry & Behavioral Sciences, Stanford University School of Medicine, Stanford, CA 94305, USA*
[b] *Department of Radiology, Stanford University School of Medicine, Stanford, CA 94305, USA*
[c] *Program in Neuroscience, Stanford University School of Medicine, Stanford, CA 94305, USA*
[d] *Stanford Brain Research Center, Stanford University School of Medicine, Stanford, CA 94305, USA*

Received 9 January 2002; revised 13 August 2002; accepted 5 November 2002

Abstract

Previous studies comparing fMRI data acquired at 1.5 T and higher field strengths have focused on examining signal increases in the visual and motor cortices. No information is, however, available on the relative gain, or the comparability of data, obtained at higher field strengths for other brain regions such as the prefrontal and other association cortices. In the present study, we investigated fMRI activation at 1.5 and 3 T during visual perception, visuospatial working memory, and affect-processing tasks. A 23% increase in striate and extrastriate activation volume was observed at 3 T compared with that for 1.5 T during the visual perception task. During the working memory task significant increases in activation volume were observed in frontal and parietal association cortices as well as subcortical structures, including the caudate, globus pallidus, putamen, and thalamus. Increases in working memory-related activation volume of 82, 73, 83, and 36% were observed in the left frontal, right frontal, left parietal, and right parietal lobes, respectively, for 3 T compared with 1.5 T. These increases were characterized by increased activation at 3 T in several prefrontal and parietal cortex regions that showed activation at 1.5 T. More importantly, at 3 T, activation was detected in several regions, such as the ventral aspects of the inferior frontal gyrus, orbitofrontal gyrus, and lingual gyrus, which did not show significant activation at 1.5 T. No difference in height or extent of activation was detected between the two scanners in the amygdala during affect processing. Signal dropout in the amygdala from susceptibility artifact was greater at 3 T, with a 12% dropout at 3 T compared with a 9% dropout at 1.5 T. The spatial smoothness of T2* images was greater at 3 T by less than 1 mm, suggesting that the greater extent of activation at 3 T beyond these spatial scales was not due primarily to increased intrinsic spatial correlations at 3 T. Rather, the increase in percentage of voxels activated reflects increased sensitivity for detection of brain activation at higher field strength. In summary, our findings suggest that functional imaging of prefrontal and other association cortices can benefit significantly from higher magnetic field strength.

Keywords: Functional magnetic resonance imaging; 1.5 T; 3 T; Visual cortex; Frontal lobe; Parietal lobe; Amygdala

Introduction

Functional magnetic resonance imaging (fMRI) is now widely used to study brain function and dysfunction. Due to their wide availability, 1.5 T systems are currently used in a majority of fMRI studies. Increasingly, however, fMRI studies are being conducted at field strengths of 3 T or higher. Recent research has demonstrated that exquisite spatial resolution can be obtained with functional imaging at higher field strength in a manner that was not possible at 1.5 T. For example, researchers have demonstrated high-resolution maps of ocular dominance columns (Cheng et al., 2001; Menon et al., 1997) and retinotopy within the lateral geniculate nucleus (Ugurbil et al., 1999). Many of the early studies comparing brain activation at 1.5 T with higher

* Corresponding author. Program in Neuroscience and Department of Psychiatry & Behavioral Sciences, 401 Quarry Road, Stanford University School of Medicine, Stanford, CA 94305-5719, USA.
E-mail address: menon@stanford.edu (V. Menon).

1053-8119/03/$ – see front matter © 2003 Elsevier Science (USA). All rights reserved.
doi:10.1016/S1053-8119(03)00002-8

fields focused on examining signal increases in the visual (Gati et al., 1997; Turner et al., 1993) and motor (Yang et al., 1999) cortices. No information, however, is available on the relative gain, or the comparability of data, obtained at higher field strengths for regions other than the visual and motor cortices. In this study we examine qualitative and quantitative differences in the patterns of activation observed at 3 and 1.5 T during sensory, cognitive, and affect-processing tasks.

For fMRI, a major advantage of using higher fields derives from the fact that the rate of transverse relaxation, $R2^* = 1/T2^*$, scales as the square of the external magnetic field for small blood vessels and capillaries, whereas the change is linear for large blood vessels (Gati et al., 1997). Since the blood oxygen level-dependent (BOLD) contrast originates from the intravoxel magnetic field inhomogeneity induced by paramagnetic deoxyhemoglobin, higher fields should result in improved sensitivity related primarily to BOLD changes in capillary beds in response to neural activity (Kruger et al., 2001; Ugurbil et al., 1999). Thus, theoretical considerations indicate that higher fields should result in improved sensitivity and spatial specificity for detection of task-related brain activation. Furthermore, since BOLD signal changes at 1.5 T are rather small (on the order of a few percent), it is thought that higher field strengths of 3 T or more should significantly enhance the ability to reliably detect signals of interest.

Four published studies to date have directly compared changes in task-related fMRI activation at 1.5 T and higher field strengths (Gati et al., 1997; Kruger et al., 2001; Turner et al., 1993; Yang et al., 1999). Two of these studies focused on the visual cortex, one on the motor cortex, and a fourth on the visual and motor cortices. Turner et al. (1993) compared activation in the visual cortex at 1.5 and 4 T during photic stimulation and reported an increase of approximately 300% in an eight-voxel (5 mm^2) region at 4 T. More recent studies have taken scanner noise and physiological fluctuations into account and have reported more modest increase in signal. Gati et al. (1997) found a 70% increase in average percentage signal change in cortical gray matter activation during photic stimulation. Yang et al. (1999) examined activation in the motor cortex during a finger-tapping task and found that at 4 T, compared with 1.5 T, there was a 70% increase in the number of voxels activated and a 20% higher average *t* score for the activated voxels. Kruger et al. (2001) examined motor and visual cortex activation at 3 T, compared with 1.5 T. They found a 44% increase in the number of voxels activated in the primary motor cortex and 36% more voxels were activated in the visual cortex compared with activation during a checkerboard reversal task (Kruger et al., 2001). Taken together, these studies suggest that higher field strength provides an advantage for functional imaging of primary sensory and motor cortices. The extent to which signal gains of the type found in primary sensory and motor cortices might extend to association cortices, e.g., the prefrontal and parietal cortex, is not known. This is an important question to examine since fMRI is now extensively used to study cognitive function and dysfunction.

A second major issue that has not been addressed in studies to date is the comparative extent of susceptibility artifacts at higher field strengths. Susceptibility artifacts result from abrupt changes in magnetic susceptibility that occur across tissue interfaces such as the border between air-filled sinuses and brain parenchyma or between bone and brain parenchyma (Ojemann et al., 1997). Brain regions closest to such borders are especially prone to BOLD signal loss due to this artifact. Brain regions that are affected by these artifacts include the orbitofrontal cortex, hippocampus, amygdala, and anterior, inferolateral temporal pole (Devlin et al., 2000; Lipschutz et al., 2001; Ojemann et al., 1997). No study to date has examined differences in activation at different magnetic field strengths using tasks that are known to involve brain regions that are prone to susceptibility artifact.

In this study, we examined differences in activation at 1.5 and 3 T using three different tasks that are known to activate distinct brain regions. We used a visual perception task known to reliably activate striate and extrastriate cortices (DeYoe et al., 1994; Watson et al., 1993), a working memory task known to reliably activate the prefrontal and parietal association cortices (Smith and Jonides, 1997, 1998), and an affect-processing task known to reliably activate the amygdala (Breiter et al., 1996; Yang et al., 2002). A random effects model was used to examine differences in activation obtained at the two field strengths. The results of this analysis were used to isolate the precise voxels that showed statistically significant differences in activation between the two field strengths. For each task, we examined the increased sensitivity for detection of activation at 3 T; by "activation" we mean voxels for which the *z* scores exceed a specified threshold. Finally, we also examined the effect of susceptibility artifacts on amygdala activation at the two field strengths.

Materials and methods

Subjects

Fourteen right-handed subjects (aged 17–25, mean age = 21.21 years, SD = 2.16; 7 male) participated in the study after giving written informed consent. fMRI data were acquired for each subject as he or she performed three different tasks involving visual perception, working memory, and affect-processing in scanners with 1.5- and 3-T magnetic field strengths. Both task order and scanner order were randomized and counterbalanced in this within-subjects design. Each subject was presented with the same order of tasks on both scans. The length of time between data acquisition at the two scanners ranged between 7 and 10 days. No subject had movement greater than 2 mm (translation)

and 2° (rotation) during the fMRI scans; movement was determined based on the displacement and rotation needed to realign the functional images at each time point with respect to the first image.

Tasks

Visual perception task

The visual perception task consisted of experimental (E) and control (C) epochs that alternated every 20 s for six cycles. The control epoch consisted of a static black and white radial checkerboard pattern. In the experimental condition the same pattern was inverted (white sections become black, black sections become white) at a frequency of 8 Hz. In both the control and experimental conditions, subjects were instructed to passively view the checkerboard. Total length of the task was 4 min. Further details of the task have been described elsewhere (Kruger et al., 2001).

Working memory task

The working memory task consisted of six alternating experimental (E) and control (C) epochs. Each experimental and control epoch consisted of 16 stimuli presented for 500 ms each, with a 1500-ms interstimulus interval. The stimulus was the letter 'O' presented in one of nine distinct visuospatial locations in a 3×3 matrix. In the experimental epoch, subjects were instructed to respond if the stimulus was in the same location as it was two trials back. In the control epoch the subject was instructed to respond if the stimulus was in the center position. Each epoch was preceded by a 4-s instruction regarding the specific task the subject should perform. Correct response rate, incorrect response rate, false alarm rate (percentage of stimuli to which the subject responded with a button press when no response was needed), and reaction times were recorded. Further details of the task have been described elsewhere (Kwon et al., 2001; Menon et al., 2000).

Affect-processing task

Subjects viewed photographs of human faces expressing angry, fearful, and neutral emotions. Task design features include: (a) four epochs of each facial expression were presented; (b) each epoch consisted of a total of eight different faces expressing the same emotion; (c) all of the faces presented were unique, with no individual face appearing more than once during the entire presentation; (d) three 24-s passive-fixation epochs were used, one each at the beginning, middle, and end of the task; (e) each face was presented for 3 s. Subjects were asked to perform a gender discrimination task while inside the scanner; they were instructed to press the right response button for a female face and to press the left response button for a male face. Accuracy and reaction times were recorded during the scan session. Further details of the task have been described elsewhere (Yang et al., 2002).

MRI data acquisition

1.5 and 3 T

The following features were common to both 1.5- and 3-T scans. A custom-built head holder was used to prevent head movement. Twenty-eight axial slices (4 mm thick, 0.5-mm skip) parallel to the anterior and posterior commissures (AC-PC) covering the whole brain were imaged with a temporal resolution of 2 s using a T2*-weighted gradient echo spiral pulse sequence (Glover and Lai, 1998). The field of view was 200×200 mm^2, and the matrix size was 64×64, giving an in-plane spatial resolution of 3.125 mm. To reduce blurring and signal loss arising from field inhomogeneities, an automated high-order shimming method based on spiral acquisitions was used before acquiring functional MRI scans (Kim et al., 2002). The sampling bandwidth was 100 kHz at both the scanners.

To keep BOLD sensitivity and susceptibility effects in GRE imaging at the higher field unchanged, we scaled TE and the flip angle with respect to T1 and T2* properties at 1.5 and 3.0 T. This set of parameter changes between field strengths is the most appropriate, as discussed in Kruger et al. (2001). Based on measured transverse relaxation times in cortical gray matter of T2* = 65 and 49 ms at 1.5 and 3.0 T, respectively, we used TE = 40 ms for imaging at 1.5 T, and TE = 30.0 ms at 3.0 T. To use the Ernst angle at each field strength we used flip angles of 89 at 1.5 T and 80 at 3.0 T based on differences in T1 relaxation times in gray matter. Details of these and other related methodological issues are discussed in Kruger et al. (2001).

Instrumental instabilities were negligible over the period of the study. Quality assurance measurements are taken weekly at both scanners; these measurements indicate that scanner noise is much less than physiological noise. The RMS noise for a phantom scanner at 31 cm FOV was 0.12% at 1.5 T and 0.10% for 3 T, compared with RMS fluctuations of 2–3% for human physiological noise. Also, order of scanning at 1.5 and 3 T was counterbalanced across subjects, thus minimizing any effect of fluctuations in signal quality.

1.5 T

Images were acquired on a 1.5-T GE Signa scanner (LX platform) with CRM gradients (40 mT/m, SR 150 mT/m/s) using a standard GE whole-head coil. The following spiral pulse sequence parameters were used: TR = 2000 ms, TE = 40 ms, flip angle = 89°, and one interleave. To aid in the localization of functional data, a high-resolution T1-weighted spoiled grass gradient recalled (SPGR) 3D MRI sequence with the following parameters was used: 124 coronal slices 1.5 mm thick, no skip, TR = 11 ms, TE = 2 ms, and flip angle = 15°. The images were reconstructed as a $124 \times 256 \times 256$ matrix with a $1.5 \times 0.9 \times 0.9$-mm spatial resolution.

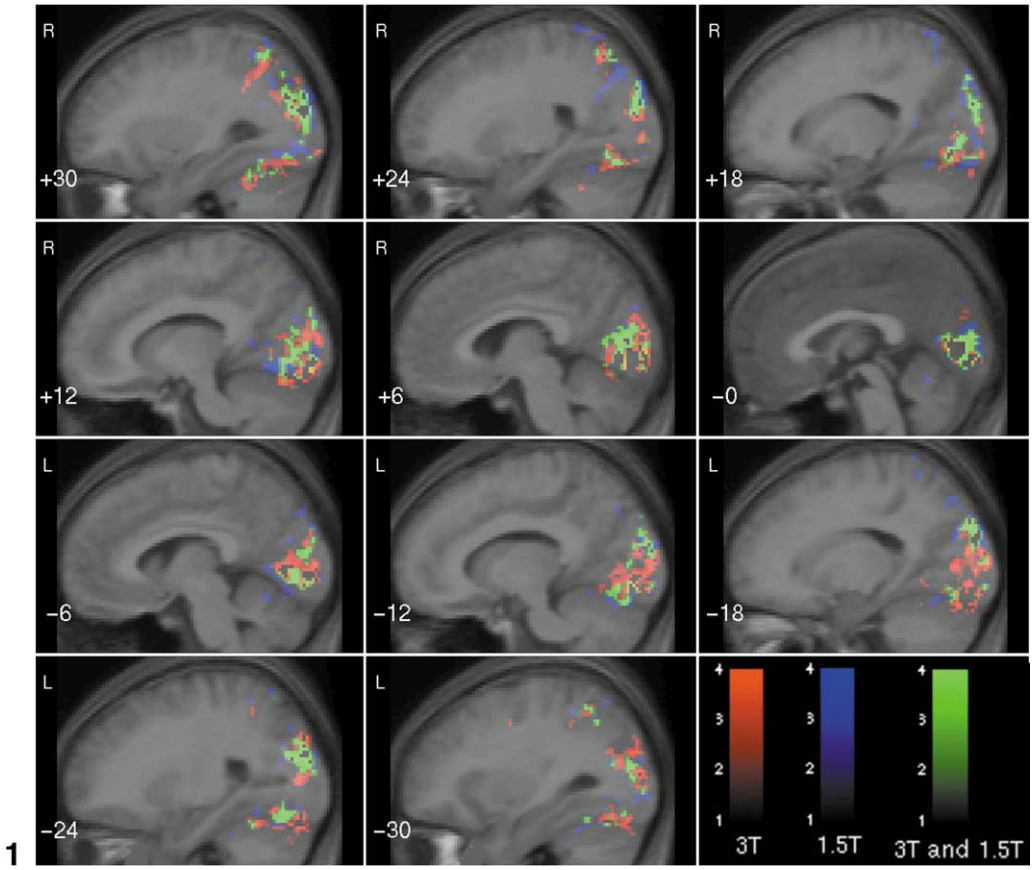

1

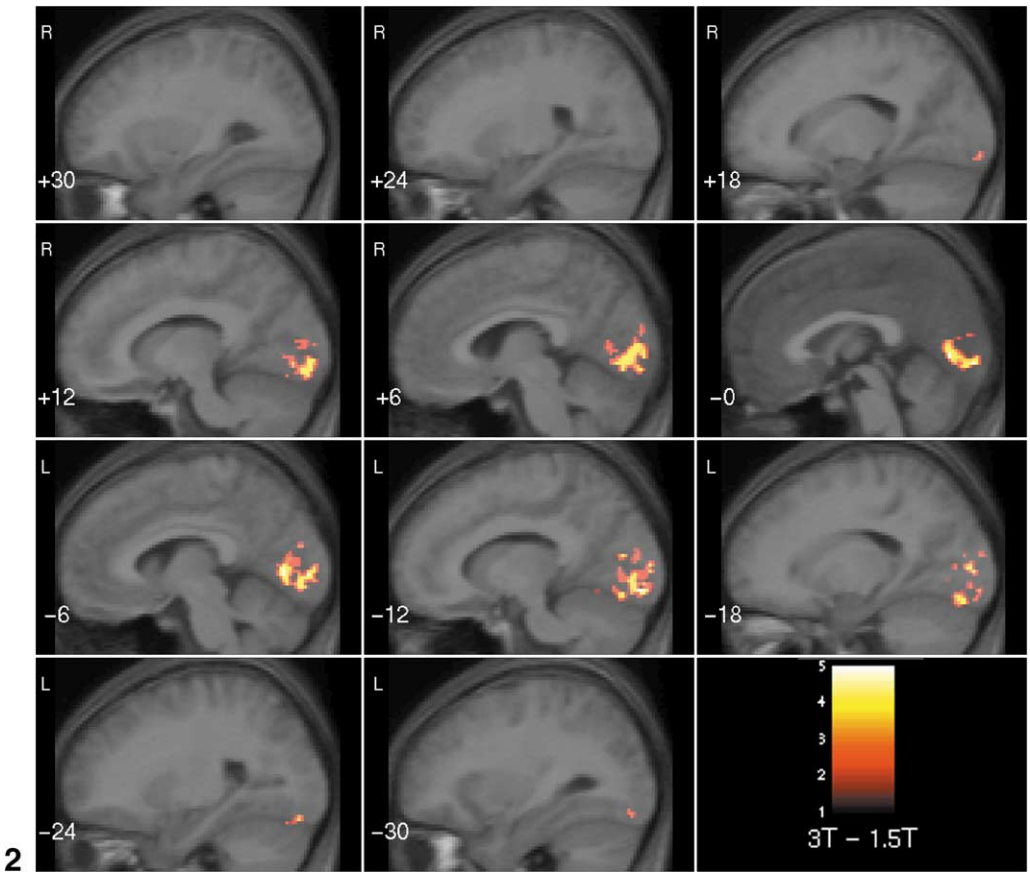

2

Fig. 1. Striate, extrastriate, and posterior parietal cortex activation during the visual perception task. Significant clusters of activation from a random effects analysis of fMRI data acquired from 14 subjects. Voxels that showed overlapping activation at 3 and 1.5 T are shown in green. Activation unique to 3 T is shown in red and activation unique to 1.5 T is shown in blue. Each activated cluster was significant after corrections for multiple spatial comparisons ($P < 0.05$). fMRI data are shown superimposed on average, spatially normalized, T1-weighted images from the same 14 subjects.

Fig. 2. Striate (V1) and extrastriate (V2 and V3) regions that showed significantly greater activation at 3 T, compared with 1.5 T, in a random effects analysis of between-scanner differences. Other details as in Fig. 1.

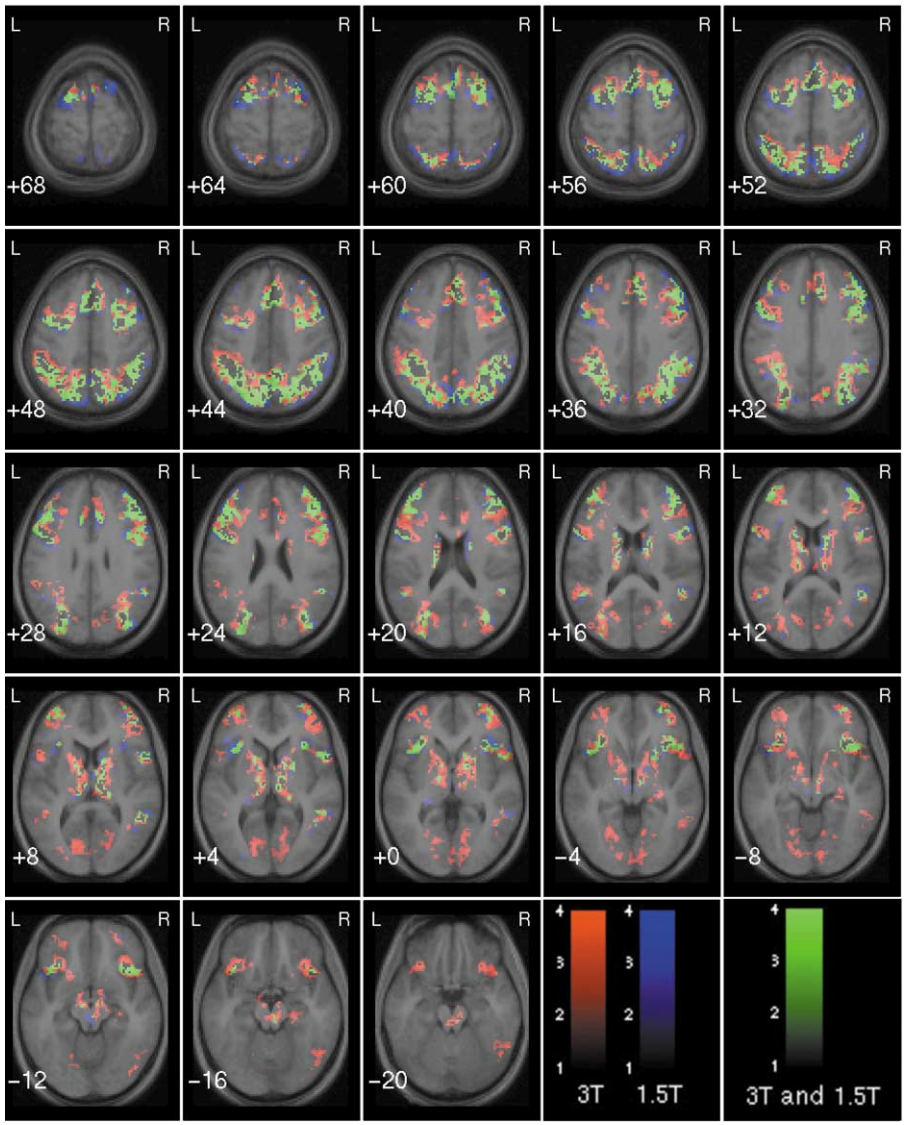

Fig. 3. Prefrontal, parietal, basal ganglia, and thalamic activation during the visuospatial working memory task. Although there is considerable overlap in activation at 3 and 1.5 T, 3-T activation was more extensive. Furthermore, several distinct regions that are not activated at 1.5 T show significant activation at 3 T. Other details as in Fig. 1.

3 T

Images were acquired on a 3-T GE Signa scanner using a standard GE whole-head coil. The scanner runs on an LX platform, with gradients in Mini-CRM configuration (35 mT/m, SR 190 mT/m/s), and has a Magnex 3-T 80-cm magnet. The following spiral pulse sequence parameters were used: TR = 2000 ms, TE = 30 ms, flip angle = 80°, and one interleave.

Stimulus presentation

The tasks were programmed using Psyscope (http://poppy.psy.cmu.edu/psyscope) on a Macintosh (Sunnyvale, CA, USA) notebook computer. Onsets of scanning and task were synchronized using a TTL pulse delivered to the scanner timing microprocessor board from a CMU Button Box' microprocessor connected to the Macintosh with a serial cable. Stimuli were presented visually at the center of a screen using a custom-built magnet-compatible projection system (1.5 T: Resonance Technology, Van Nuys, CA, USA; 3 T: Sanyo, San Diego, CA, USA).

Image preprocessing

Images were reconstructed, by inverse Fourier transform, for each time point. fMRI data were preprocessed using SPM99 (http://www.fil.ion.ucl.ac.uk/spm). Images were corrected for movement using least-squares minimization without higher-order corrections for spin history, and normalized (Friston et al., 1995b) to stereotaxic Talairach coordinates (Talairach and Tournoux, 1998). Images were then resampled every 2 mm using sinc interpolation and smoothed with a 4-mm Gaussian kernel to decrease spatial noise.

fMRI data analysis

Statistical analysis was performed on individual and group data using the general linear model and the theory of Gaussian random fields as implemented in SPM99 (Friston et al., 1995a). This method takes advantage of multivariate regression analysis and corrects for temporal and spatial autocorrelations in the fMRI data. Activation foci were superimposed on high-resolution T1-weighted images and their locations interpreted using known neuroanatomical landmarks (Duvernoy et al., 1999).

A within-subjects procedure was used to model all the effects of interest for each subject. Individual subject models were identical across subjects (i.e., a balanced design was used). Confounding effects of fluctuations in global mean were removed by proportional scaling where, for each time point, each voxel was scaled by the global mean at that time point. Low-frequency noise was removed with a high-pass filter (0.5 Hz) applied to the fMRI time series at each voxel. We then defined the effects of interest for each subject with the relevant contrasts of the parameter estimates.

Group analysis was performed using a random-effects model that incorporated a two-stage hierarchical procedure. This model estimates the error variance for each condition of interest across subjects, rather than across scans (Holmes and Friston, 1998), and therefore provides a stronger generalization to the population from which data are acquired. This analysis proceeded in two steps. In the first step, contrast images for each subject and each effect of interest were generated as described above. In the second step, these contrast images were analyzed using a general linear model to determine voxelwise t statistics. Contrast images were computed for experimental minus control conditions for each task at the two field strengths. Appropriate t-tests were then used to determine (i) group activation at 3 T, (ii) group activation at 1.5 T, and (iii) differences in activation between 3 and 1.5 T. Finally, the t statistics were normalized to Z scores, and significant clusters of activation were determined using the joint expected probability distribution of height and extent of Z scores, with height ($Z > 1.67$, $P < 0.05$) and extent ($P < 0.05$) thresholds (Poline et al., 1997).

To quantify changes in sensitivity for detection of activation at 3 T, we first determined the number of voxels that showed significant between-scanner differences (using comparison iii above) in task-relevant brain regions. This number divided by the number of voxels that were activated at 1.5 T in these same regions was used as the measure of the increased sensitivity for detection of activation at 3 T. Task-specific regions of interest included (1) striate and extrastriate cortex for the visual perception task, (2) frontal lobe (Brodmann's areas (BAs) 6, 8, 9, 44, 45, 46, 11, 47) and parietal lobe (BA 7, 40, 39) for the working memory task, and (3) the amygdala for the affect-processing task.

ROI analysis

For further analysis of the working memory task, we used the automated parcellation scheme of Tzourio-Mazoyer et al. (2002) to demarcate regions of interest in the prefrontal and parietal cortices and the cerebellum. The percentage of voxels activated and mean Z scores were computed for each region at 1.5 and 3 T.

For analysis of the affect-processing task, amygdala ROIs were demarcated separately in the left and right hemispheres on T1-weighted spatially normalized images. ROIs were drawn for each individual subject using a reliable protocol that has been described in detail elsewhere (Kates et al., 1997). Briefly, amygdala ROIs were drawn on coronal slices, beginning on the slice where the anterior commissure first crosses the midline of the brain. ROIs were drawn beginning inferolaterally, moving medially to the border between the amygdala and the white matter tract inferior to it. The medial border of the ROI was drawn at the CSF/gray border. The ROI continued superomedially to the gray/white border and around the lateral amygdala to the starting point. In the posterior regions of the amygdala, the superior border was partially defined by the presence of the enthorinal sulcus.

To statistically compare activation across facial expressions and hemispheres in the amygdala, a repeated-measures ANOVA was conducted with factors of hemisphere (left, right) and affect (anger vs neutral, and fear vs neutral). A standard analysis framework was employed in which the percentage voxels activated and the average Z scores of activated voxels in each ROI were used as measures of activation. An α of $P < 0.05$ (two-tailed) was used as the threshold for statistical significance.

Assessing susceptibility artifacts

Signal loss due to susceptibility artifacts was quantified by counting the percentage of voxels within the amygdala that had an intensity below a prespecified threshold. For each subject, we approximated the threshold masking procedure used in SPM99 by first eliminating all voxels whose T2* intensity in the averaged smoothed image was less than one-eighth of the global mean. The mean of the remaining voxels was used as a second threshold such that any voxels below this mean were also eliminated. In the subsequent statistical analyses performed by SPM, these voxels are labeled NaN (not a number) on contrast images and have a t score of 0 on the statistical maps. Further details of this analysis and its application to susceptibility artifact detection are described elsewhere (Greicius et al., 2003). The percentage of voxels with signal dropout was computed for each individual subject using T2* images acquired at 3 and 1.5 T. Between-scanner differences were examined using ANOVA with factors magnetic field strength (3 T, 1.5 T) and hemisphere (left, right). To visualize the precise location of the signal dropout within the amygdala, a composite image of voxels with signal dropout was computed by averaging across all 14 subjects.

Smoothness of T2 images*

The smoothness (spatial correlation) of T2* images was determined using the methods described by Kiebel et al. (1999) and the procedures implemented in SPM99. Briefly, this involves computing the determinant of the covariance matrix of the first spatial partial derivatives of the residual field derived after removing task-specific and nonspecific physiological noise components (e.g., low-frequency drifts). The inverse of the determinant is the spatial smoothness of the fMRI data. Spatial smoothness of images acquired at 3 and 1.5 T was compared using two-tailed paired *t* tests.

Results

Visual perception task

Activation

Significant activation was observed in the striate, extrastriate, and posterior parietal cortex at both 3 and 1.5 T, with more extensive activation at 3 T (Fig. 1). A direct comparison of activations using random effects analysis revealed a greater number of activated voxels at 3 T in the striate cortex (VI) and extrastriate regions (V2 and V3) (Fig. 2). Significant between-scanner differences were detected in 896 voxels; 3811 voxels were activated at 1.5 T, implying an increase in activation of 23.5%.

No regions showed greater activation at 1.5 T compared with 3 T.

Smoothness of T2 images*

The average smoothness of the images was 5.56 ± 0.45 mm at 1.5 T and 6.34 ± 0.45 mm at 3 T. The smoothness at 3 T was significantly greater ($t(12) = 6.67$, $P < 0.00002$).

Working memory task

Behavioral performance

There were no significant differences in accuracy or reaction times obtained at the two scanners. Mean accuracy on the working memory task was 90.5 ± 3.6 and 91.8 ± 2.7% in the 1.5- and 3-T scanners, respectively. Mean reaction times were 688.0 ± 148.7 and 682.5 ± 141.5 ms in the 1.5- and 3-T scanners, respectively.

Activation

The extent of working memory-related activation was greater at 3 T in the left and right frontal and parietal lobes (Fig. 3). A direct statistical comparison showed a greater number of activated voxels at 3 T bilaterally in the superior, middle, and inferior frontal gyri, orbital gyrus, supplementary motor area (SMA), pre-SMA, superior and inferior parietal lobules, as well as cerebellum (Larsell region HVIIB), caudate head, globus pallidus, and thalamus (Fig. 4). The percentage increase in activation was approximately 82% in the left frontal lobe (% increase = 100 × 3852/4700; 3852 voxels were activated in the 3 T–1.5 T comparison, 4700 voxels were activated at 1.5 T), 73% (4635/6324) in the right frontal lobe, 83% (3494/4208) in the left parietal lobe, and 36% (1825/5129) in the right parietal lobe.

We examined the distribution of *Z* scores in voxels that showed significant activation at 3 T. Figure 5 compares the distribution of *Z* scores for these voxels at the two field strengths. The distributions were significantly different (Kolmogorov–Smirnov test, $D = 0.521174$, $P < 0.001$) with means of −0.202 ± 2.093 at 1.5 T and 2.658 ± 1.932 at 3 T, and kurtosis of 0.13 at 1.5 T and 0.49 at 3 T.

Figure 6 shows the percentage of voxels activated and mean *Z* scores at 1.5 and 3 T in specific prefrontal, parietal, and cerebellar regions of interest during the working task. Activation increases were significant ($P < 0.01$) in all regions shown.

Smoothness of T2 images*

The average smoothness of the images was 5.68 ± 0.57 mm at 1.5 T and 6.49 ± 0.62 mm at 3 T. The smoothness at 3 T was significantly greater ($t(13) = 3.04$; $P < 0.0095$).

Affect-processing task

Behavioral performance

Mean accuracy on the tasks was 92.4 ± 5.4 and 93.9 ± 4.4% in the 1.5- and 3-T scanners, respectively. Mean reaction times were 892.7 ± 166.8 and 849.4 ± 130.7 ms in the 1.5- and 3-T scanners, respectively. There were no significant differences in accuracy or reaction times obtained at the two scanners.

Amygdala activation

Amygdala activation in response to emotional, compared with neutral, faces was observed at both 3 and 1.5 T. Between-scanner differences were detected in eight voxels in the amygdala, with greater activation at 3 T, compared with 1.5 T. This difference was, however, not significant when a small volume correction was applied.

To further quantify between-scanner differences in activation an ROI analysis was also performed. A 2 (field strength: 3 T, 1.5 T) × 2 (hemisphere: left, right) repeated-measures ANOVA was used to directly contrast the extent and magnitude of activation in the amygdala. There was no significant main effect of field strength ($F(1,13) = 0.050$, $P = 0.826$) or significant interaction between field strength and hemisphere ($F(1,13) = 0.514$, $P = 0.486$) (Fig. 7). Nearly identical results were found for average *Z* scores of suprathreshold voxels ($Z > 0.05$) in the amygdala.

Signal dropout in amygdala

Of the 468 voxels in the left amygdala, 9.8 ± 7.0% voxels showed signal dropout from susceptibility artifacts at 1.5 T, compared with 11.3 ± 6.4% at 3 T; of the 458 voxels in the right amygdala, 8.4 ± 5.2% voxels showed signal dropout from susceptibility artifacts at 1.5 T, compared with 13.2 ± 5.4% at 3 T (Fig. 8). Figure 9 shows the precise regions in the

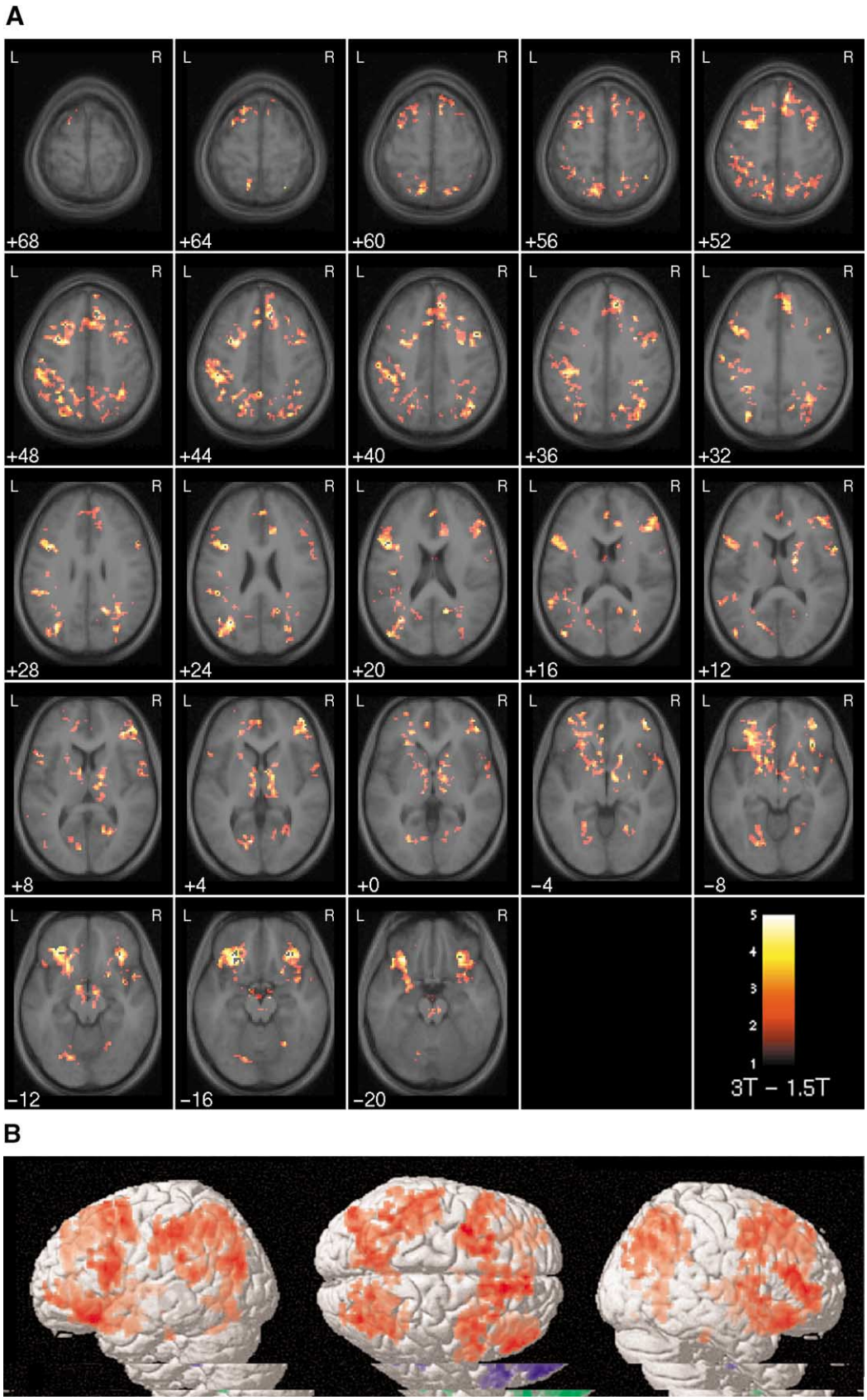

Fig. 4. Brain regions that showed significantly greater activation at 3 T, compared with 1.5 T, in a random effects analysis of between-scanner differences during the working memory task: (A) coronal cross sections, (B) surface rendering. Greater activation was observed in the prefrontal and parietal cortex as well as subcortical structures including the caudate, putamen, and thalamus.

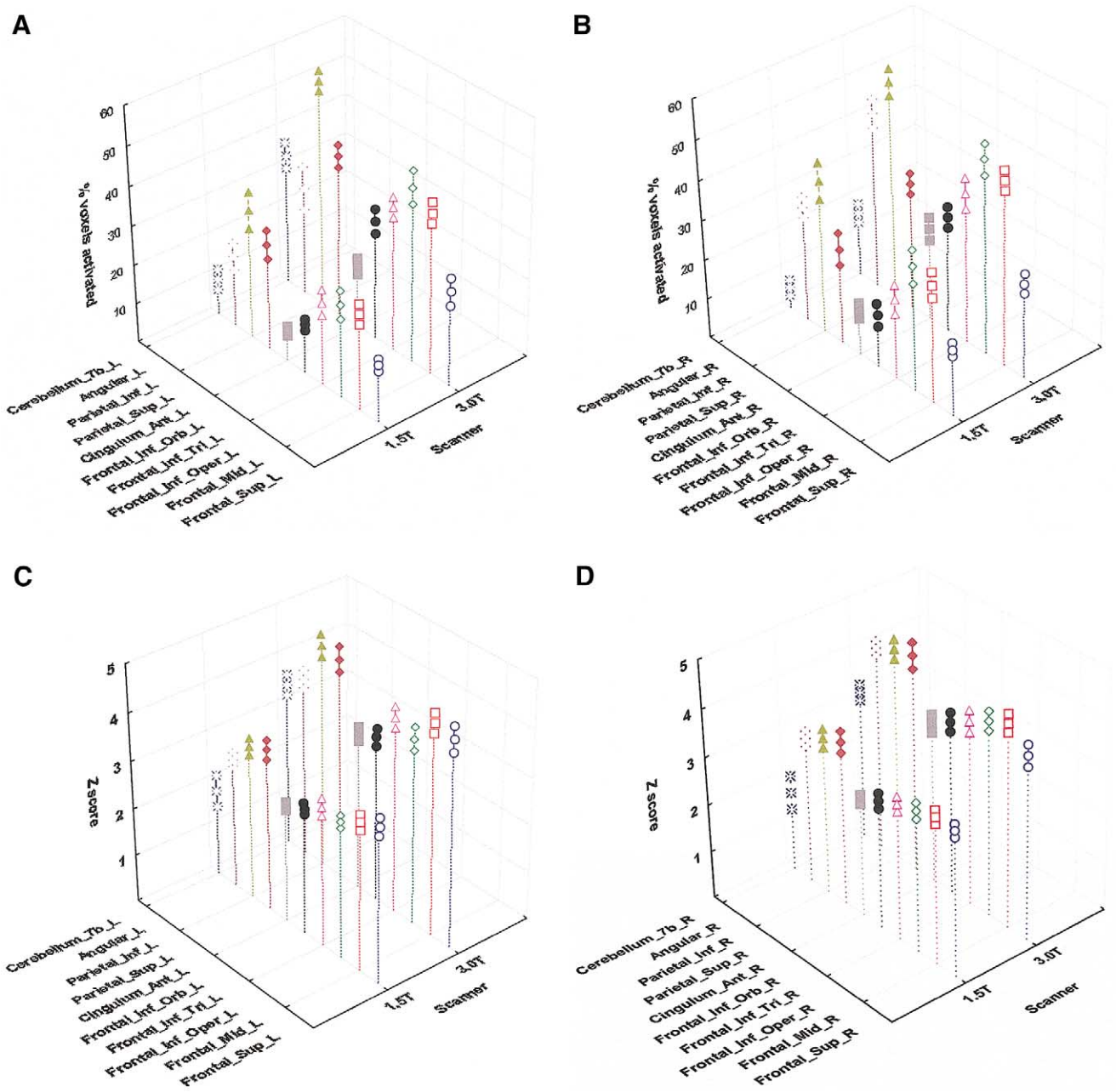

Fig. 6. Percentages of voxels activated (A, B) and mean *Z* scores (C, D) at 1.5 and 3 T in specific prefrontal, parietal, and cerebellar regions of interest during the working task. Activation increases were significant in all regions shown. Left and right hemisphere regions are shown on the left and right, respectively. The automated parcellation scheme of Tzourio-Mazoyer et al. (2002) was used to demarcate regions of interest: Frontal_Sup, superior frontal gyrus; Frontal_Mid, middle frontal gyrus; Frontal_Inf_Oper, inferior frontal gyrus, opercular part; Frontal_Inf_Tri, inferior frontal gyrus, triangular part; Frontal-_Inf_Orb, Inferior frontal gyrus, orbital part; Cingulum_Ant, anterior cingulate cortex; Parietal_Inf, inferior parietal cortex (sans supramarginal and angular gyri); Angular, angular gyrus; Cerebellum_7B, Larsell's cerebellar region HVIIB.

amygdala where signal dropout was observed in all 14 subjects. Analysis of variance revealed a trend toward greater signal dropout at 3 T ($F(1, 13) = 4.528$, $P = 0.053$), and there was no significant interaction between field strength and hemisphere ($F(1, 13) = 2.875$, $P = 0.114$).

Amygdala activation after adjusting for signal dropout

When the ROI analysis of amygdala activation during affect processing was restricted to artifact-free voxels, no significant main effect of field strength or interaction between field strength and hemisphere emerged.

Discussion

During both the visual perception and visuospatial working memory tasks significantly greater cortical activation was observed at 3 T, compared with 1.5 T. Increased acti-

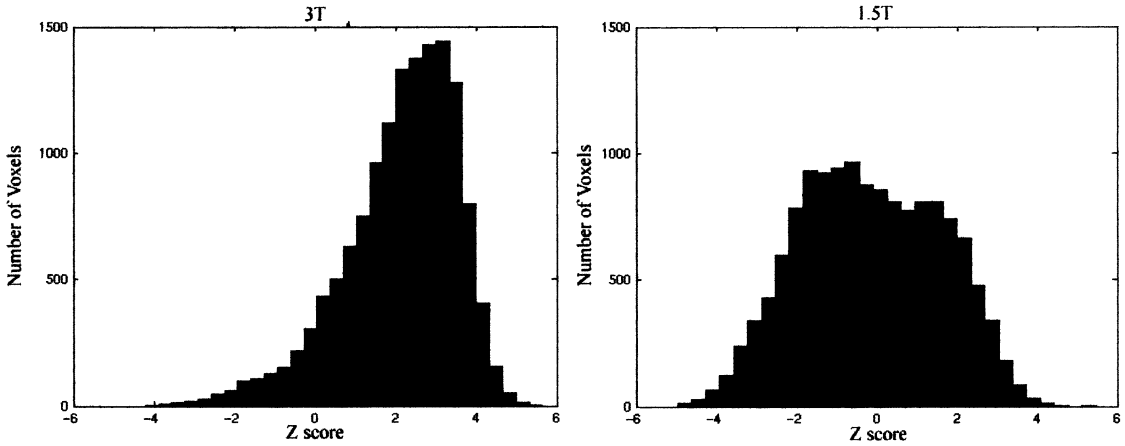

Fig. 5. Distribution of *Z* scores at 3 and 1.5 T among voxels that showed significant activation at 3 T during the working memory task. The distributions were significantly different with means of -0.202 ± 2.093 at 1.5 T and 2.658 ± 1.932 at 3 T, and kurtosis of 0.13 at 1.5 T and 0.49 at 3 T.

vation at 3 T was most dramatic in frontal and parietal cortices during the working memory task. Compared with an increase in visual cortex activation of about 23% during the visual perception task, increases in activated voxels of 78% in the prefrontal cortex and 59% in the parietal cortex were observed during the working memory task. In contrast, amygdala activation during the affect-processing task was not significantly different at 3 and 1.5 T.

We used identical tasks, data acquisition procedures, and a counterbalanced design in which the same subjects were scanned at both 3 and 1.5 T, thus minimizing the effects of habituation and learning on differences in activation. The fairly large number of subjects and use of a random effects analysis provide better generalizability and localization of activation differences than has been possible in previous studies. The measure used to examine increased sensitivity for detection of activation at 3 T captures (1) voxels that may not have been activated at 1.5 T, which show significant activation at 3 T, as well as (2) voxels that activated at 1.5 T, which show statistically significant increases in activation at 3 T. The increased volume of activation at 3 T may, therefore, arise either from differences in extent of activation or from changes in the height of activation or both. Our measure therefore provides a more sensitive gauge of voxelwise changes at 3 T than simply comparing the number of voxels that were activated (above a specified threshold) at the two field strengths.

Our results clearly indicate that the increase in regional activation at 3 T extends across several centimeters of the cortex in one or more directions. In comparison, the spatial smoothness, or intrinsic spatial correlation, increased by less than 1.4 mm at 3 T. The smoothness was assessed on residual fields that are free of physiological signal, thus allowing one to estimate the smoothness of the resulting *t* field under the null hypothesis of no activation (Kiebel et al., 1999). These observations suggest that the more extensive activation observed at 3 T may arise from increased vascular (presumably venous vessel) contributions to the BOLD signal (Kruger et al., 2001); however, since the density and distribution of vessels of various sizes were not studied here we do not know whether the intermediate vessels sizes were particularly heterogeneous across the size scales of the relatively large imaging voxels.

The extent of spatial smoothing used in our study is modest considering that data were acquired with a resolution close to 4 mm. This level of smoothing essentially removes spatial noise and, to a lesser extent, reduces the effects of anatomical variability across subjects. Our results clearly show that the spatial extent of activation differences at 1.5 and at 3 T extends to several centimeters, far in excess of the extent of spatial smoothing used. Changes in activation were detected even in regions where 1.5 T provides enough sensitivity to significantly activate voxels corresponding to active neuronal tissue. Furthermore, rather than merely reflecting "volume of activation" changes, our results also show that at 3 T we can detect significant activation in neuroanatomically distinct brain regions that were not activated at 1.5 T.

We used a shorter TE at 3 T to compensate for shorter T2* at 3 T. The shorter T2* can lead to increased spatial blurring on the Fourier-transformed images. Although in general shorter T2* leads to increased spatial blurring, the effect can be shown to be very small in our case, as the readout duration was only about 20 ms for both field strengths due to the high efficiency of the spiral acquisition method. Our analysis suggests that the intrinsic spatial correlations increase by only about 1 mm at 3 T, whereas the spatial extent of activation increases over several centimeters. This suggests that the increased activation at 3 T arises at least partly from increased signal at 3 T, rather than increased spatial blurring. Furthermore, the distribution of *Z* scores within regions above threshold at 3 T was significantly different from the distribution at 1.5 T, with significantly greater means at 3 T.

Our data also contribute to an understanding of the important problem of false negatives (type II error) in analyses

with thresholding as is performed in SPM. If we were to assume that all voxels present at 3 T represent true positives (or at least the majority of the voxels that differ by field strength) we would have to assume a very high false negative rate. This problem, of course, could not be unqiue to 1.5 T—the higher-field instrument will also show false negatives. While there is no gold standard for true positive activations and the fMRI design by itself cannot distinguish between type I and type II error, converging evidence from lesion and electrophysiological studies suggests that most of the activations that were observed only at 3 T represent type II error in 1.5-T data.

Our data demonstrate that 3 T shows greater activation in striate and extrastriate regions. Regions of the extrastriate cortex that showed increases in activation include V2 and V3, regions known to be involved in real and illusory motion perception. Furthermore, these increases are reliable across subjects as indicated by the random effects analysis of fMRI data in the present study. The increased activation at 3 T in both striate and extrastriate regions should allow for increasingly more sophisticated analyses of visual processing systems (Somers et al., 1999).

Compared with the 23% increase in activation of primary and secondary visual cortex observed during the visual perception task at 3 T, more striking increases of 35–83% were observed in association cortices during the working memory task. Within the prefrontal and parietal cortices, increases in activation were observed in both hemispheres in specific regions that are known to play critical roles in working memory (Nystrom et al., 2000; Postle et al., 2000). Moreover, activation in these regions is more extensive than what has been previously reported. The parallel increases in activation of these regions are consistent with the involvement of frontoparietal loops in working memory (Smith and Jonides, 1998) and with electrophysiological studies that have shown that the prefrontal and parietal cortices are coactivated during working memory (Chafee and Goldman-Rakic, 1998). A direct comparison of activation at 3 and 1.5 T revealed greater bilateral activation at 3 T in the dorsolateral prefrontal cortex, inferior frontal gyrus, orbital gyrus, supplementary motor area, inferior parietal cortex, cerebellum, caudate, globus pallidus, putamen, and thalamus. Our results, therefore, suggest that higher field strength is particularly advantageous for the study of not only cortical, but also subcortical, contributions to higher cognitive function. Furthermore, at 3 T, activation was detected in several brain regions that did not show significant activation at 1.5 T. Prominent among these regions are the ventral aspects of the inferior frontal gyrus, orbitofrontal gyrus in the prefrontal cortex, and the lingual gyrus in the temporal-occipital cortex. The precise role of these regions in working memory is now the subject of intense investigation; a discussion of these issues in beyond the scope of our study. What is important to note here is that higher field strength, in any case 3 T, will facilitate a more thorough quantification of overlapping as well as distributed representations of neural processes involved in higher cognitive functions (Duncan and Owen, 2000; Halgren et al., 2002). This in turn should help in resolving controversies regarding domain- and process-specific functional organization of the prefrontal and other association cortices (Goldman-Rakic, 2000; Miller, 2000).

In contrast to these findings, no increase in amygdala activation at 3 T was observed during affect processing. Furthermore, signal dropout from susceptibility artifacts was greater at 3 T, with dropout regions extending more laterally in comparison to amygdala regions that showed dropout at 1.5 T. However, even when the analysis was restricted to voxels that did not have a significant dropout, no differences in activation were found at 3 and 1.5 T. This finding suggests either that signal gain in the amygdala is small or that signal reductions may extend beyond the dropout regions that have been identified in the present study. In either case, there appears to be little difference between detectable activation at 1.5 and 3 T in the amygdala. Deichmann et al., (2002) argue that susceptibility effects may cause changes in BOLD sensitivity over and above the results of dropout, due to local variations in effective echo time (Deichmann et al., 2002). This may explain the findings described here. The basal nucleus and the adjoining peri-amygdaloid cortex (Olmos, 1990) are the main amygdala regions affected by susceptibility artifact. This region is known to play a key role in attaching emotional significance to stimuli. Furthermore, by means of the ventral amygdalofugal pathway, these regions project to the medial dorsal nucleus, the thalamic relay nucleus for association areas in the frontal lobe. There is also considerable evidence that the basal nucleus is involved in associating sensory cues with reward value (Baxter and Murray, 2002; Cardinal et al., 2002). Thus, signal loss in this region may adversely affect the analysis and interpretation of amygdala function.

The amygdala has been a difficult structure to image with fMRI (Merboldt et al., 2001; Yang et al., 2002) and findings about its role in different aspects of affect processing have been quite variable across studies. For example, most studies have found amygdala activation in response to fearful faces (Baird et al., 1999; Hariri et al., 2000; Phillips et al., 1998; Whalen et al., 1998). However, an fMRI study at 2 T found no amygdala activation in response to fearful faces (Sprengelmeyer et al., 1998). For other facial emotions such as anger, sadness, and happiness, the fMRI studies regarding amygdala activation have been even more variable (Breiter et al., 1996; Hariri et al., 2000; Phillips et al., 1998; Schneider et al., 1997; Sprengelmeyer et al., 1998). More importantly, in the present study we found that there was an equally large variance in activation across subjects at 1.5 and 3 T. Together these results indicate that BOLD signals are small and highly variable across subjects in the amygdala even at 3 T; significant technical improvements are therefore necessary to improve signal detection in this brain region, and thereby facilitate the resolution of existing con-

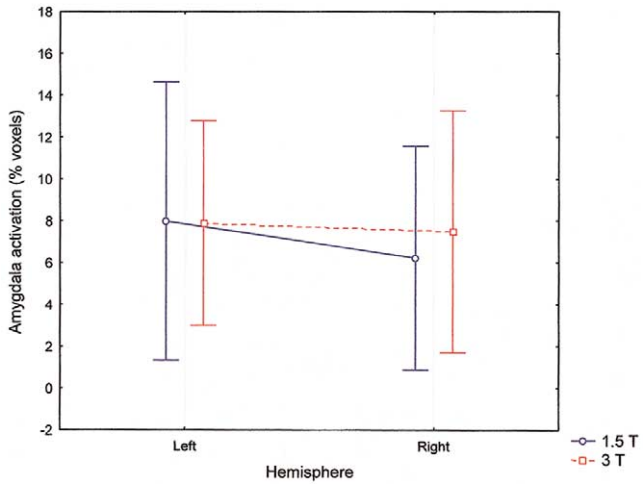

Fig. 7. Amygdala activation during the affect-processing task was not significantly different at 3 and 1.5 T. Vertical bars denote 0.95 confidence intervals. Note the large variance in activation across subjects at both 3 and 1.5 T.

troversies regarding the precise role of the human amygdala in affect processing.

More broadly, similar arguments are likely to extend to other brain regions, such as the anterior hippocampus, anterior temporal pole, and inferior orbitofrontal cortex, which are also affected by susceptibility artifacts. For echo-planar imaging, the sensitivity to BOLD effects appears to be directly proportional to signal intensity (Lipschutz et al., 2001); this suggests that BOLD signal detection can be reduced even in the absence of complete signal dropout. In summary, in regions such as the amygdala, there is a trade-off between signal gain due to higher field strength and loss due to susceptibility artifacts.

Our findings demonstrate that 3 T is generally more

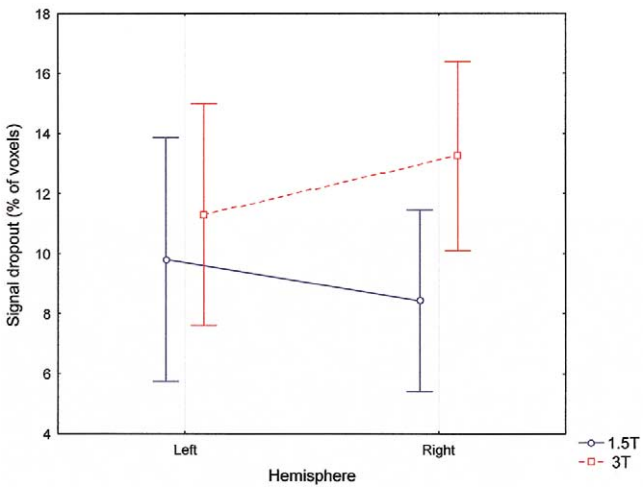

Fig. 8. Percentage of voxels in amygdala that showed signal dropout from susceptibility artifacts. Greater dropout was observed at 3 T, with larger effects in the right hemisphere. Vertical bars denote 0.95 confidence intervals.

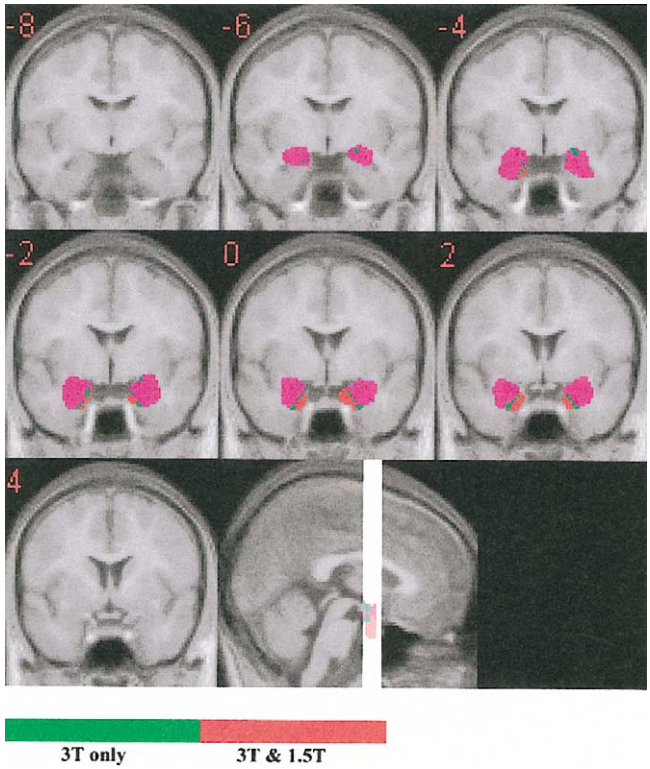

Fig. 9. Coronal views of amygdala regions that showed signal dropout due to susceptibility artifacts; the last viewgraph shows a sagittal view of the locations of these slices. The Talairach coordinate of each coronal slice is shown in the top left-hand corner. The basal nucleus and the adjoining peri-amygdaloid cortex are the main amygdala regions affected by susceptibility artifact. Voxels with signal dropout at both 3 and 1.5 T are shown in red; voxels that showed dropout at 3 T but not at 1.5 T are shown in green. Voxels in purple did not show dropout at either 3 or 1.5 T. Regions with dropout are shown superimposed on average, spatially normalized, T1-weighted images from 14 subjects.

advantageous than 1.5 T for functional brain imaging. This advantage extends beyond the primary visual and motor cortices to association cortices, including the dorsolateral prefrontal and inferior parietal cortices, as well as subcortical structures, including the striatum and thalamus. Higher-field magnet strength does not, however, guarantee uniformly superior functional imaging results. In particular, susceptibility artifacts are greater at 3 T and this has adverse effects on detection of any potential increases in task-related activation in regions such as the amygdala. These effects are also likely to be a significant confounding factor in the interpretation of hippocampal activation during episodic memory, an issue that is discussed in detail elsewhere (Greicius et al., 2003). Improvements in high-field instrumentation and better pulse sequences are essential for fMRI applications that use high fields (Ugurbil et al., 1999); in particular, future technological investigations need to focus on reducing the susceptibility artifacts at high field to maximize the benefits of high field scanning (Cordes et al., 2000). It is possible that magnetic field strengths higher than 3 T will produce greater signal and further improve the

spatial resolution of fMRI (Yacoub et al., 2001). However, as the present study indicates, there is likely to be a trade-off with respect to the extent of susceptibility artifacts that can be tolerated. Future studies will address differences in task-related *decreases* in activation, or deactivation (Raichle et al., 2001).

Acknowledgments

This research was supported by NIH Grants HD40761, MH62430, RR09784, and MH19908, and grants from the Norris Foundation, and the Lucas Imaging Center.

References

Baird, A.A., Gruber, S.A., Fein, D.A., Maas, L.C., Steingard, R.J., Renshaw, P.E., 1999. Functional magnetic resonance imaging of facial affect recognition in children and adolescents. J. Am. Acad. Child Adolesc. Psychiatry 38, 195–199.

Baxter, M.G., Murray, E.A., 2002. The amygdala and reward. Nat. Rev. Neurosci. 3, 563–573.

Breiter, H., Etcoff, N.L., Whalen, P.J., Kennedy, W.A., Rauch, S.L., Buckner, R.L., 1996. Response and habituation of the human amygdala during visual processing of facial expression. Neuron 17, 875–887.

Cardinal, R.N., Parkinson, J.A., Hall, J., Everitt, B.J., 2002. Emotion and motivation: the role of the amygdala, ventral striatum, and prefrontal cortex. Neurosci. Biobehav. Rev. 26, 321–352.

Chafee, M.V., Goldman-Rakic, P.S., 1998. Matching patterns of activity in primate prefrontal area 8a and parietal area 7ip neurons during a spatial working memory task. J. Neurophysiol. 79, 2919–2940.

Cheng, K., Waggoner, R.A., Tanaka, K., 2001. Human ocular dominance columns as revealed by high-field functional magnetic resonance imaging. Neuron 32, 359–374.

Cordes, D., Turski, P., Sorenson, J., 2000. Compensation of susceptibility-induced signal loss in echo-planar imaging for functional applications. Magn. Reson. Imaging 18, 1055–1068.

Deichmann, R., Josephs, O., Hutton, C., Corfield, D.R., Turner, R., 2002. Compensation of susceptibility-induced BOLD sensitivity losses in echo-planar fMRI imaging. NeuroImage 15, 120–135.

Devlin, J., Russell, R., Davis, M., Price, C., Wilson, J., Moss, H., 2000. Susceptibility-induced loss of signal: comparing PET and fMRI on a semantic task. NeuroImage 11, 589–600.

DeYoe, E.A., Bandettini, P., Neitz, J., Miller, D., Winans, P., 1994. Functional magnetic resonance imaging (FMRI) of the human brain. J. of Neurosci. Methods 54, 171–187.

Duncan, J., Owen, A.M., 2000. Common regions of the human frontal lobe recruited by diverse cognitive demands. Trends Neurosci. 23, 475–483.

Duvernoy, H.M., Bourgouin, P., Cabanis, E.A., Cattin, F., 1999. The Human Brain: Functional Anatomy, Vascularization and Serial Sections with MRI. Springer-Verlag, New York.

Friston, K.J., Holmes, A.P., Worsley, K.J., Poline, J.P., Frith, C.D., Frackowiak, R.S.J., 1995a. Statistical parametric maps in functional imaging: a general linear approach. Hum. Brain Mapp. 2, 189–210.

Friston, K.J., Frith, C.D., Poline, J.B., Heather, J.D., Frackowiak, R.S.J., 1995b. Spatial registration and normalization of images. Hum. Brain Mapp. 2, 165–189.

Gati, J.S., Menon, R.S., Ugurbil, K., Rutt, B.K., 1997. Experimental determination of the BOLD field strength dependence in vessels and tissue. Magn. Reson. Med. 38, 296–302.

Glover, G.H., Lai, S., 1998. Self-navigated spiral fMRI: interleaved versus single-shot. Magn Reson Med 39, 361–368.

Goldman-Rakic, P., 2000. Localization of function all over again. NeuroImage 11, 451–457.

Greicius, M., Krasnow, B., Boyett, J.M., Eliez, S., Schatzberg, A.F., Reiss, A.L., Menon, V., 2003. Regional analysis of hippocampal activation during encoding and retrieval: an fMRI study. Hippocampus 13, 164–174.

Halgren, E., Boujon, C., Clarke, J., Wang, C., Chauvel, P., 2002. Rapid distributed fronto-parieto-occipital processing stages during working memory in humans. Cereb. Cortex 12, 710–728.

Hariri, A.R., Bookheimer, S.Y., Mazziotta, J.C., 2000. Modulating emotional responses: effects of a neocortical network on the limbic system. NeuroReport 11, 43–48.

Holmes, A.P., Friston, K.J., 1998. Generalizability, random effects, and population inference. NeuroImage 7, 754.

Kates, W.R., Abrams, M.T., Kaufmann, W.E., Breiter, S.N., Reiss, A.L., 1997. Reliability and validity of MRI measurement of the amygdala and hippocampus in children with fragile X syndrome. Psychiatry Resv75, 31–48.

Kiebel, S.J., Poline, J.B., Friston, K.J., Holmes, A.P., Worsley, K.J., 1999. Robust smoothness estimation in statistical parametric maps using standardized residuals from the general linear model. NeuroImage 10, 756–766.

Kim, D.H., Adalsteinsson, E., Glover, G., Spielman, D., 2002. Regularized higher-order in vivo shimming. Magn. Reson. Med. 48, 715–722.

Kruger, G., Kastrup, A., Glover, G.H., 2001. Neuroimaging at 1.5 T and 3.0 T: comparison of oxygenation-sensitive magnetic resonance imaging. Magn. Reson. Med 45, 595–604.

Kwon, H., Menon, V., Eliez, S., Warsofsky, I.S., White, C.D., Dyer-Friedman, J., 2001. Functional neuroanatomy of visuospatial working memory in fragile X syndrome: relation to behavioral and molecular measures. Am. J. Psychiatry 158, 1040–1051.

Lipschutz, B., Friston, K., Ashburner, R., Turner, R., Price, C., 2001. Assessing study-specific regional variations in fMRI signal. NeuroImage 13, 392–398.

Menon, V., Kwon, H., Eliez, S., Taylor, A.K., Reiss, A.L., 2000. Functional brain activation during cognition is related to FMR1 gene expression. Brain Res. 877, 367–370.

Menon, R.S., Ogawa, S., Strupp, J.P., Ugurbil, K., 1997. Ocular dominance in human V1 demonstrated by functional magnetic resonance imaging. J. Neurophysiol. 77, 2780–2787.

Merboldt, K.D., Fransson, P., Bruhn, H., Frahm, J., 2001. Functional MRI of the human amygdala? NeuroImage 14, 253–257.

Miller, E.K., 2000. The prefrontal cortex: no simple matter. NeuroImage 11, 447–450.

Nystrom, L.E., Braver, T.S., Sabb, F.W., Delgado, M.R., Noll, D.C., Cohen, J.D., 2000. Working memory for letters, shapes, and locations: fMRI evidence against stimulus-based regional organization in human prefrontal cortex. NeuroImage 11, 424–446.

Ojemann, J.G., Akbudak, E., Snyder, A.Z., McKinstry, R.C., Raichle, M.E., Conturo, T.E., 1997. Anatomic localization and quantitative analysis of gradient refocused echo-planar fMRI susceptibility artifacts. NeuroImage 6, 156–167.

Olmos, J., 1990. Amygdaloid nuclear gray complex, in G. Paxinos (Ed.), Human Nervous System, Academic Press, San Diego.

Phillips, M.L., Young, A.W., Scott, S.K., Calder, A.J., Andrew, C., Giampietro, V., 1998. Neural responses to facial and vocal expressions of fear and disgust. Proc. R. Soc. London Ser. B 265, 1809–1817.

Poline, J.B., Worsley, K.J., Evans, A.C., Friston, K.J., 1997. Combining spatial extent and peak intensity to test for activations in functional imaging. NeuroImage 5, 83–96.

Postle, B.R., Stern, C.E., Rosen, B.R., Corkin, S., 2000. An fMRI investigation of cortical contributions to spatial and nonspatial visual working memory. NeuroImage 11, 409–423.

Raichle, M.E., MacLeod, A.M., Snyder, A.Z., Powers, W.J., Gusnard, D.A., Shulman, G.L., 2001. A default mode of brain function. Proc. Natl. Acad. Sci. USA 98, 676–682.

Schneider, F., Grodd, W., Weiss, U., Klose, U., Mayer, K.R., Nagele, T., 1997. Functional MRI reveals left amygdala activation during emotion. Psychiatry Res. 76, 75–82.

Smith, E.E., Jonides, J., 1997. Working memory: a view from neuroimaging. Cogn. Psychol. 33, 5–42.

Smith, E.E., Jonides, J., 1998. Neuroimaging analyses of human working memory. Proc. Natl. Acad. Sci. USA 95, 12061–12068.

Somers, D.C., Dale, A.M., Seiffert, A.E., Tootell, R.B., 1999. Functional MRI reveals spatially specific attentional modulation in human primary visual cortex. Proc. Natl. Acad. Sci. USA 96, 1663–1668.

Sprengelmeyer, R., Rausch, M., Eysel, U.T., Przuntek, H., 1998. Neural structures associated with recognition of facial expressions of basic emotions. Proc. R. Soc. London Ser. B 265, 1927–1931.

Talairach, J., Tournoux, P., 1998. Co-planar Stereotaxic Atlas of the Human Brain. Thieme Medical, New York.

Turner, R., Jezzard, P., Wen, H., Kwong, K.K., Le Bihan, D., Zeffiro, T., 1993. Functional mapping of the human visual cortex at 4 and 1.5 tesla using deoxygenation contrast EPI. Magn. Reson. Med. 29, 277–279.

Tzourio-Mazoyer, N., Landeau, B., Papathanassiou, D., Crivello, F., Etard, O., Delcroix, N., 2002. Automated anatomical labeling of activations in SPM using a macroscopic anatomical parcellation of the MNI MRI single-subject brain. NeuroImage 15, 273–289.

Ugurbil, K., Hu, X., Chen, W., Zhu, X.H., Kim, S.G., Georgopoulos, A., 1999. Functional mapping in the human brain using high magnetic fields. Philos. Trans. R. Soc. London Ser. 354, 1195–1213.

Watson, J.D., Myers, R., Frackowiak, R.S., Hajnal, J.V., Woods, R.P., Mazziotta, J.C., 1993. Area V5 of the human brain: evidence from a combined study using postiron emission tomography and magnetic resonance imaging. Cereb. Cortex. 3, 79–94.

Whalen, P.J., Rauch, S.L., Etcoff, N.L., McInerney, S.C., Lee, M.B., Jenike, M.A., 1998. Masked presentations of emotional facial expressions modulate amygdala activity without explicit knowledge. J. Neurosci. 18, 411–418.

Yacoub, E., Shmuel, A., Pfeuffer, J., Van De Moortele, P.F., Adriany, G., Andersen, P., 2001. Imaging brain function in humans at 7 Tesla. Magn. Reson. Med. 45, 588–594.

Yang, T.T., Menon, V., Eliez, S., Gotlib, I., Reiss, A.L., 2002. Amygdala is activated by faces with positive and negative affect: evidence from high-resolution 3T scanning. NeuroReport 13, 1737–1741.

Yang, Y., Wen, H., Mattay, V.S., Balaban, R.S., Frank, J.A., Duyn, J.H., 1999. Comparison of 3D BOLD functional MRI with spiral acquisition at 1.5 and 4.0 T. NeuroImage 9, 446–451.